down to $L/d \sim 10$. The present work theoretically substantiates their finding and suggests even a wider range of applicability (down to $L/d \sim 4$) of the Yamakawa–Fujii formula for Ξ of the wormlike cylinder.

Appendix

We wish to calculate Ξ_0 for the straight touched beads model, using the same Oseen–Burgers procedure as for continuous models. The equation derived by Fujita (eq 7 in ref 14) for the beads model is pertinent to this purpose. When the Kirkwood–Riseman approximation[15] is used, it gives

$$3\pi\eta_0 nd/\Xi_0 = 1 + (d/2n)\sum_{i\neq j}\sum \langle 1/R_{ij}\rangle \qquad \text{(A1)}$$

for a straight rod composed of n touched spherical beads of diameter d. Here $\langle 1/R_{ij}\rangle$ is the mean reciprocal distance between the ith and the jth beads. Introduction of the relation $\langle 1/R_{ij}\rangle = (|j - i|d)^{-1}$ into eq A-1, followed by summation, gives

$$3\pi\eta_0 nd/\Xi_0 = \psi(n + 1) + \gamma \qquad \text{(A2)}$$

where γ is the Euler constant equal to 0.5772 and ψ is defined by

$$\psi(z) = \frac{d}{dz} \ln \Gamma(z)$$

Since $\psi(n + 1) = \ln n + 1/(2n) - 1/(12n^2) + 1/(120n^4) + \ldots$ for $n >> 1$, replacement of nd by L yields

$$3\pi\eta_0 L/\Xi_0 = \ln (L/d) + 0.5772 + (1/2)(d/L) - (1/12)(d/L)^2 + (1/120)(d/L)^4 + \ldots \qquad \text{(A3)}$$

References and Notes

(1) O. B. Ptitsyn and Yu. E. Eizner, *Vysokomol. Soedin.*, **3**, 1863 (1961).
(2) J. E. Hearst and W. H. Stockmayer, *J. Chem. Phys.*, **37**, 1425 (1962).
(3) A. Peterlin, *J. Polym. Sci.*, 8, 173 (1952).
(4) R. Ullman, *J. Chem. Phys.*, **53**, 1734 (1970).
(5) H. Yamakawa and M. Fujii, *Macromolecules*, **6**, 407 (1973).
(6) O. Kratky and G. Porod, *Recl. Trav. Chim. Pays-Bas*, **68**, 1106 (1949).
(7) S. Broersma, *J. Chem. Phys.*, **32**, 1632 (1960).
(8) T. Norisuye, H. Murakami, and H. Fujita, *Macromolecules*, **11**, 966 (1978).
(9) C. W. Oseen, "Hydrodynamik", Akademische Verlagsgesellschaft, Leipzig, 1927.
(10) J. M. Burgers, "Second Report on Viscosity and Plasticity of the Amsterdam Academy of Sciences", Nordemann, New York, 1938, Chapter 3.
(11) F. Perrin, *J. Phys. Radium*, **7**, 1 (1936).
(12) V. A. Bloomfield, K. E. Van Holde, and W. O. Dalton, *Biopolymers*, **5**, 149 (1967).
(13) M. T. Record, Jr., C. B. Woodbury, and R. B. Inman, *Biopolymers*, **14**, 393 (1975).
(14) H. Fujita, *J. Polym. Sci., Polym. Phys. Ed.*, 11, 899 (1973).
(15) J. G. Kirkwood and J. Riseman, *J. Chem. Phys.*, **16**, 565 (1948).

Surface Studies on Multicomponent Polymer Systems by X-ray Photoelectron Spectroscopy. Polystyrene/Poly(ethylene oxide) Diblock Copolymers

H. Ronald Thomas* and James J. O'Malley

Xerox Corporation, Webster Research Center, Rochester, New York 14644.

Received July 13, 1978

ABSTRACT: X-ray photoelectron spectroscopy (XPS) is a surface characterization technique capable of providing detailed information about the structure and bonding of molecules in the solid state. In this study, we have used XPS to elucidate the surface topography and copolymer composition of a series of polystyrene/poly(ethylene oxide) diblock copolymer thin films at the polymer–air interface. These copolymers undergo microphase separation when solvent cast into films. The XPS results clearly indicate that the copolymer compositions of the surfaces (e.g., outermost ~50 Å) are significantly different from the overall bulk compositions. Surface excesses of polystyrene are observed in all copolymer films cast from chloroform, ethylbenzene, and nitromethane. Angular dependent XPS studies [XPS(θ)] support a model for the topography of the copolymer surfaces that has isolated domains of each homopolymer at the surface appearing thick on the XPS scale of ~50 Å with a fractional area coverage proportional to the mole percent bulk composition of the copolymers.

The application of X-ray photoelectron spectroscopy (XPS) to the study of polymer surfaces has been pioneered by Clark and co-workers over the past few years.[1-3] The inherent surface sensitivity (top few tens of angstroms) of XPS enables one to differentiate the surface from the subsurface structure and bonding in particular systems. Simply, the XPS experiment involves the measurement of binding energies of electrons ejected by interactions of a molecule with a monoenergetic beam of soft X-rays.[4] The surface sensitivity and the capability of differentiating the surface from subsurface are a consequence of the extremely short (<100 Å) mean free paths (λ) of electrons and their strong dependence on kinetic energy.[5] By taking advantage of (1) the differences in λ associated with electrons from different core levels in the same or different atoms and (2) angular XPS studies [XPS(θ)],[3] it is possible to depth profile the compositional variations in the surfaces of solids.

In this work we have utilized XPS to investigate the influence of chemical composition and film casting solvent on the surface structure of polystyrene (PS)–poly(ethylene oxide) (PEO) diblock copolymers. Earlier studies[6,7] of the bulk morphologies and properties of the copolymers indicated that the PS and PEO components are highly incompatible and that they readily undergo microphase separation and domain formation. These studies also showed that the bulk morphology of the copolymer films was profoundly influenced by the solvent from which the films were cast. On the other hand, there have been no investigations of the surface properties of these copolymers and, in particular, their surface composition and topography at the air–copolymer interface. We can anticipate, however, that the surface and the bulk will not be identical because of the significant differences in the solid state surface tension of PS (36 dyn/cm)[8] and PEO (44 dyn/cm).[8] The XPS studies have indeed revealed significant dif-

0024-9297/79/2212-0323$01.00/0 © 1979 American Chemical Society

Table I
Bulk Compositions and Number Average Molecular Weights for the Three PS/PEO Diblock Copolymers

sample	% PS wt	% PS mol	$\bar{M}_n \times 10^{-3}$ (by membrane osmometry) PS-PEO
A	19.6	9.6	21.2-87.2
B	39.3	21.4	13.2-20.3
C	70.0	49.5	24.3-10.4

ferences between the surface and bulk properties of these copolymers but, more importantly, the ability to measure the angular dependence of the spectra [XPS(θ)] has enabled us to propose and test models for the topography of the copolymer films.

Experimental Section

A. Samples. (i) Styrene/Ethylene Oxide Diblock Copolymer Samples. The block copolymers were prepared by a two-stage anionic polymerization technique and purified to remove unwanted homopolymers by fractional precipitation from selected solvents under controlled conditions. The synthesis and characterization of these PS–PEO diblock copolymers has been described in detail elsewhere.[9] The bulk compositions and number average molecular weights are shown in Table I.

(ii) Homopolymers. The homopolymers used as references in the XPS study included polystyrene prepared by a standard anionic polymerization technique, purified by precipitation into hexane, and recovered as a fine powder. The poly(ethylene oxide) homopolymer (Union Carbide "Carbowax" 25K $\bar{M}_w$) was received in flake form and no further purification was performed.

B. XPS Sample Preparation. The three copolymers were obtained for XPS analysis as fine powders and were studied as thin films prepared by dip coating from dilute solutions of the appropriate solvents [spectroscopic grade chloroform (Burdick and Jackson), reagent grade nitromethane (Eastman Kodak) and ethylbenzene (Eastman Kodak)] onto flat aluminum substrates. The samples were dried in an Argon atmosphere at ambient temperature to reduce surface oxidation of the copolymers and thick coatings were obtained by multiple dipping to insure the substrate Al_{2p} core level signals were attenuated to an unobservable level. No annealing or time (i.e., aging) effects were studied on the samples.

C. XPS Instrumentation. Spectra were recorded on an AEI ES200B spectrometer by using Mg $K\alpha_{1,2}$ exciting radiation. Typical operating conditions were: X-ray gun, 12 kV, 15 mA; pressure in the source chamber ca. 10^{-8} torr. Under the experimental conditions employed, the gold $4f_{7/2}$ level at 84 eV binding energy (BE) used for calibration had a full-width half-maximum (FWHM) of 1.2 ± 0.1 eV. No evidence was obtained for radiation damage to the sample from long-term exposure to the X-ray beam. Due to the rather long analysis times required for the angular dependent studies a liquid-nitrogen-cooled X-ray cap was used throughout the study to eliminate hydrocarbon contamination of the sample surface and this device has been described in detail elsewhere.[10]

Calibration of the absolute energy scale was achieved by disconnecting the liquid-nitrogen-cooling cap on the X-ray anode and allowing hydrocarbon contamination to collect on the sample surface. The value of 285.0 eV was used for the C_{1s} core level of the hydrocarbon and the details of this method of calibration have been discussed elsewhere.[3]

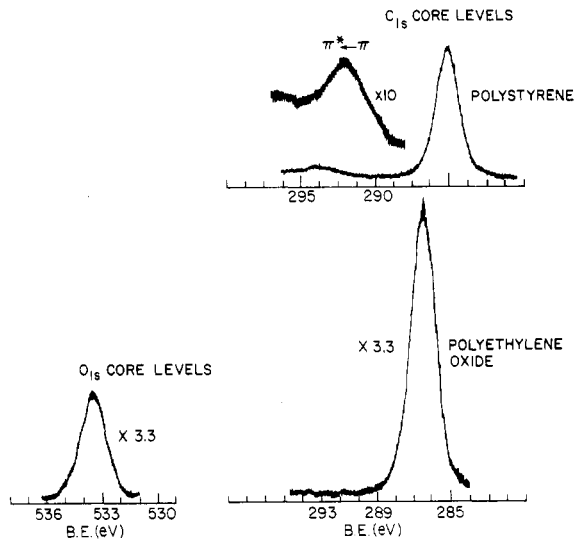

Figure 1. C_{1s} and O_{1s} core level spectra for polystyrene and poly(ethylene oxide) homopolymers.

Overlapping peaks were resolved into their individual components by use of a DuPont 310 curve resolver (an analog computer). The detailed deconvolutions were based on a knowledge of line widths determined from studies of homopolymers and model compounds.[11] These studies have shown that for individual components of the core level spectra for C_{1s} and O_{1s} levels, the line shapes are approximately Gaussian.

Results

Homopolymers. In order to establish a firm basis for the interpretation of the diblock copolymer data, it is necessary to study the component homopolymers, polystyrene (PS) and poly(ethylene oxide) (PEO), and determine their absolute and relative binding energies and relative peak intensities. The XPS core level spectra for PS and PEO are shown in Figure 1 and the experimental binding energies and peak intensity ratios are tabulated in Table II.

The PS spectrum has a strong peak centered at 285 eV associated with the direct photoionization of the C_{1s} core levels and a low-energy satellite peak at 291.6 eV arising from shake-up transitions ($\pi^* \leftarrow \pi$) accompanying core ionization. These low-energy shake-up transitions are understood both theoretically and experimentally and the spectrum observed in Figure 1 is entirely consistent with previous work.[12-17] The spectra for PEO show a single peak for the C_{1s} levels at 286.5 eV, referenced to hydrocarbon at 285 eV, and a single peak for the O_{1s} core levels at 533.3 eV. The peak area ratio of the C_{1s} to O_{1s} core levels is 0.73; however, when these peak areas are corrected for the different theoretical photoionization cross sections[18] and electron mean free paths[5] relative to the C_{1s} and O_{1s} core level electrons the correct stoichiometry for PEO is obtained.

The chemical shift of ~1.5 eV for the C_{1s} core level peak in PEO, relative to PS, can be attributed to each carbon being attached to an oxygen atom and is consistent with

Table II
Experimental Binding Energies and Peak Area Ratios for the Reference Homopolymers, Polystyrene and Poly(ethylene oxide)

	binding energy,[a] C_{1s}	$C_{1s}(\pi^* \leftarrow \pi)$	O_{1s}	peak area ratios
polystyrene	285.0	291.6		$C_{1s}(PS)/C_{1s}(PEO) = 1.60 \pm 0.1$
poly(ethylene oxide)	286.5		533.3	$C_{1s}(PEO)/O_{1s}(PEO) = 0.73 \pm 0.05$
				$C_{1s}(\pi^* \leftarrow \pi)(PS)/C_{1s}(PS) = 0.081 \pm 0.005$

[a] Referenced to hydrocarbon at 285.0 eV.

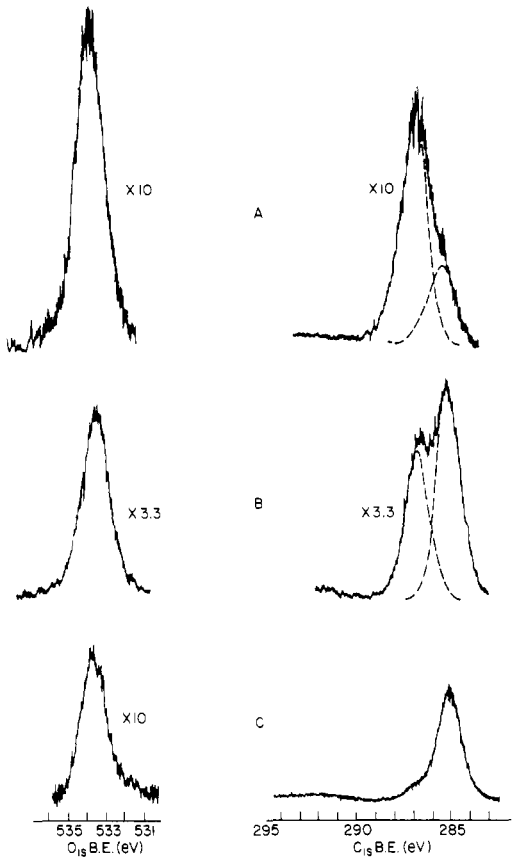

Figure 2. C_{1s} and O_{1s} core level spectra for the three PS/PEO diblock copolymers cast from chloroform.

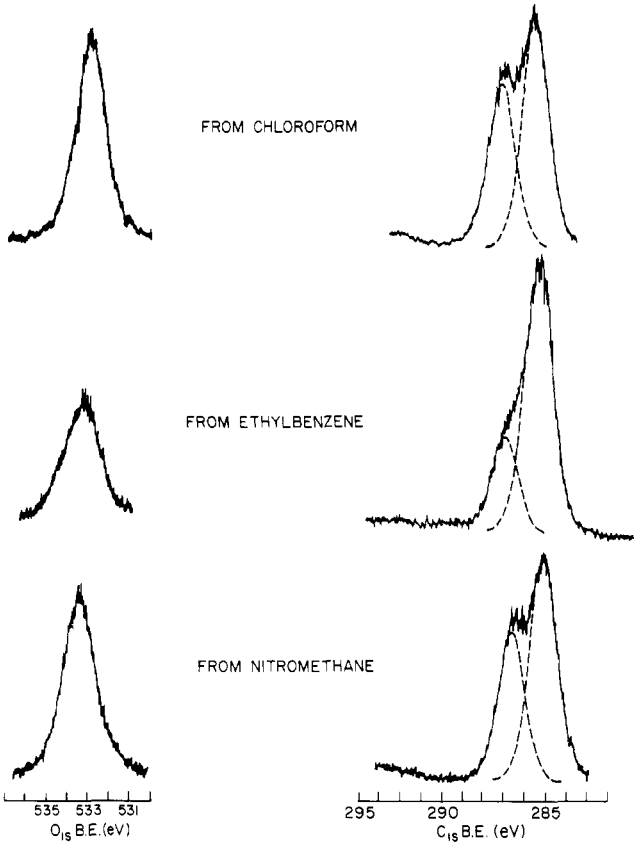

Figure 3. C_{1s} and O_{1s} core level spectra for the PS/PEO diblock copolymer (B) cast from chloroform, ethylbenzene, and nitromethane.

theoretical predictions and experimental results on related low-molecular-weight model compounds.[11,19] As expected, there is no shake-up peak in the C_{1s} core level spectrum for PEO since the polymer is fully saturated.[3] These significant differences in the XPS spectra of PS and PEO, i.e., the 1.5 eV chemical shift in the C_{1s} core levels, the uniqueness of the $\pi^* \leftarrow \pi$ shake-up peak associated with the PS component, coupled with the peak intensity ratios from Table II, enable a unique analysis of the surface composition of the PS/PEO system.

PS-PEO Diblock Copolymers

Films of the three block copolymers were cast from chloroform, a mutual solvent for PS and PEO,[6] and the measured C_{1s} and O_{1s} core level spectra are shown in Figure 2. The spectra show the characteristic O_{1s} peak of PEO, the shake-up satellite of PS, and an easily deconvoluted doublet for the C_{1s} core levels in PS and PEO. It is apparent from the spectra that the PS concentration at the copolymer surface increases as the PS in the copolymer increases. More importantly, however, an analysis of the spectral data clearly shows that the surface compositions are significantly richer in PS than would be predicted based on a knowledge of the bulk compositions of the block copolymers.

Earlier work on these copolymers[6] established that varying the film-casting solvent had a profound influence on sample morphology as determined by optical and electron microscopies. Therefore, we decided to determine if these morphological changes were accompanied by changes in surface composition as measured by XPS. Copolymer films were cast from ethylbenzene, a preferential solvent for PS, nitromethane, a preferential solvent for PEO, and chloroform, a mutual solvent. An example of the C_{1s} and O_{1s} core level spectra taken for one of the copolymers (sample B) cast from these three solvents is shown in Figure 3. It is immediately apparent that the surface composition of the diblock copolymer varies significantly as a function of the casting solvent. The PS content at the copolymer surface increases as the solvent becomes more preferential for PS and with ethylbenzene one finds the extraordinary result that the surface composition is about 70% PS whereas the bulk composition is only 21.4 mol % PS.

In Figure 4 are shown the surface vs. bulk composition data for the three block copolymers cast from the three solvents. The trends in surface vs. bulk compositions are the same for all three copolymers when the films are cast from the aforementioned solvents.

Angular Dependent XPS Studies. Depth Profiling Surfaces

Up to this point all the XPS measurements have been made by analyzing the photoemitted electrons normal to the surface of the sample under investigation. This experimental arrangement is the most commonly used in XPS studies, and with it the effective sampling depth is maximized. For systems such as PS/PEO, the effective sampling depth is about 50 Å; i.e., about 95% of the signal comes from the outermost ~50 Å, based upon a previous knowledge of the electron mean free paths appropriate to photoemitted electrons from the C_{1s} (~960 eV) and O_{1s} (~720 eV) core levels.[5] Therefore, the surface composition data shown in Figure 4 are the average composition on this effective sampling depth of ~50 Å.

These measurements can be further refined by controllably decreasing the effective sampling depth. This will, in effect, allow for depth profiling the composition of the upper 50 Å of the surface and provide us with a means to explore the molecular organization of the surface

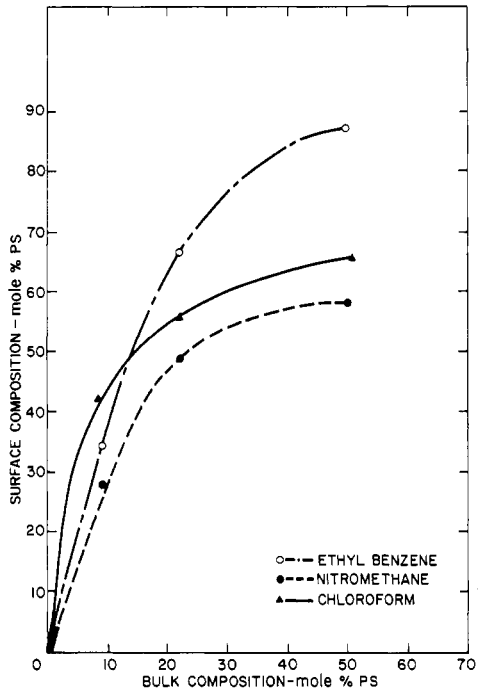

Figure 4. Surface vs. bulk compositions as a function of solvent and copolymer composition.

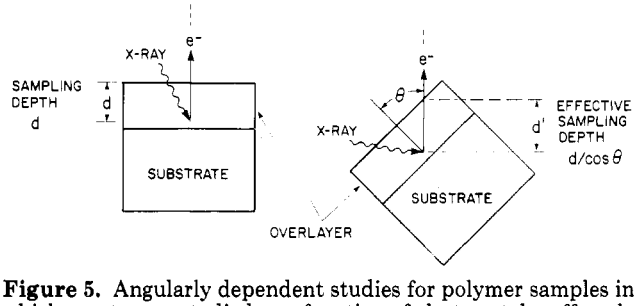

Figure 5. Angularly dependent studies for polymer samples in which spectra are studied as a function of electron take-off angle θ with respect to the sample surface.

macromolecules. The method for varying the effective sampling depth is shown schematically in Figure 5. The sample is rotated relative to the fixed position energy analyzer by angle θ, designated as the angle between the normal to the sample and the slits in the analyzer. It is readily seen that electrons collected at grazing exit angles relative to the surface ($\theta \rightarrow 90°$) will enhance surface features relative to electrons collected normal to the surface.[3,5,20]

In Figure 6 are shown the C_{1s} and O_{1s} core level spectra from the angular dependent XPS studies, [XPS(θ)], on copolymer B cast from chloroform. Spectra were recorded at three different angles, θ = 0, 45, and 80°, in order to achieve effective sampling depths of ~50, ~25, and ~10 Å, respectively. Both the C_{1s} and O_{1s} core level spectra clearly show that each component of the copolymer is present at all sampling depths. Furthermore, from the relative intensity ratios of the deconvoluted C_{1s} peaks associated with the PS and PEO components, we find that in particular cases, there is a concentration gradient in the top 50 Å of the surface and that the relative concentration of PS to PEO increases as the air–solid polymer interface is approached.

Similar spectra were recorded for the other block copolymers as a function of take-off angle (θ) and film casting solvent, and Table III contains the tabulated copolymer compositions at the various sampling depths. An appreciable surface excess of PS, relative to the bulk, is found

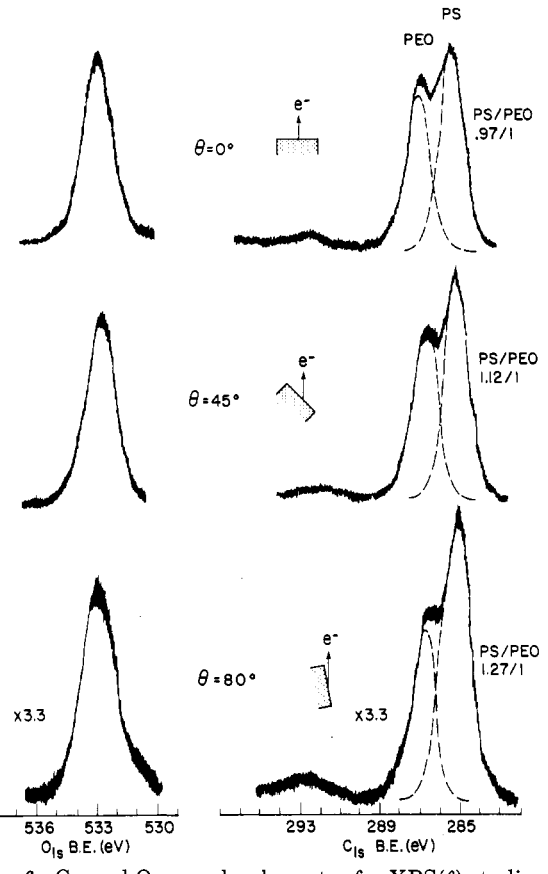

Figure 6. C_{1s} and O_{1s} core level spectra for XPS(θ) studies on PS/PEO diblock copolymer (B) cast from chloroform. The experimental intensity ratios are corrected for absolute signal from Table II to obtain the molar ratios.

Table III
Copolymer Compositions of the PS/PEO Diblock Copolymers Calculated from the XPS Data as a Function of Casting Solvent and Sampling Depth

sample	mol % of PS at surface		
	θ = 0°	θ = 45°	θ = 80°
A (chloroform)	42	54	62
B (chloroform)	46	52	56
C (chloroform)	82	85	86
A (ethylbenzene)	34	38	46
B (ethylbenzene)	67	71	74
C (ethylbenzene)	88	86	88
A (nitromethane)	28	28	29
B (nitromethane)	50	52	55
C (nitromethane)	59	58	72

at all sampling depths and the surface excess is largest at θ = 80° where the effective sampling depth is ~10 Å. Not all of the sample films, however, exhibit a composition gradient over the top 50 Å. Films cast from solvents preferential for the major component in the copolymer do not show any significant angular dependence in the composition. Conversely, there is an angular dependence in films cast from solvents preferential for the minor component in the copolymer and from the mutual solvent, chloroform. In these systems, the gradient in composition is relatively small and gradual.

Measurements of the signal intensities of the C_{1s} and O_{1s} peaks of the PEO component of the copolymers were also made during the XPS(θ) study. As will be discussed later, the C_{1s}/O_{1s} peak area ratios for PEO in the copolymer are important in a proposed model for the copolymer surfaces. In this study, the C_{1s}/O_{1s} ratio remained invariant with

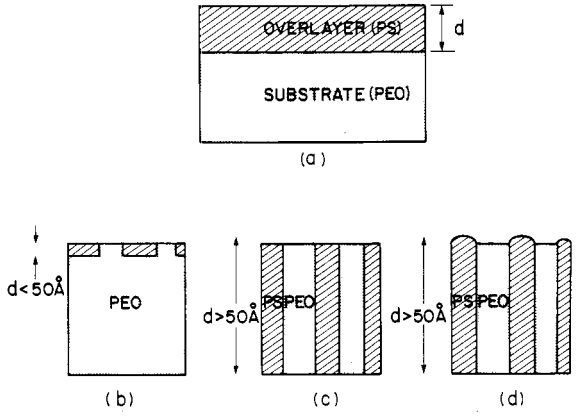

Figure 7. Models for the surface topography of the PS/PEO diblock copolymers.

changing angle θ, except for a film of copolymer C cast from nitromethane where it increased slightly as θ was increased.

Discussion

In this section we present various models for the topography of the block copolymers, and we will use the experimental results to test their applicability. The well-known continuous overlayer model[21,22] as well as alternate models based on discontinuous, heterogeneous surfaces will be proposed and evaluated. The models to be discussed are shown in Figure 7.

The lateral and vertical homogeneity of a sample can best be explored by XPS(θ) studies when the sample contains core levels which have significantly different electron mean free paths for the photoemitted electrons.[3] The intensity of a signal coming from a given core level can be expressed in terms of the two basic equations for signal attenuation given below

$$I_i^{\circ} = f_i(\theta)F\alpha_i N_i k_i \lambda_i (1 - e^{-d/\lambda_i \cos\theta}) \quad (1)$$

$$I_j^{s} = f_j(\theta)F\alpha_j N_j k_j \lambda_j e^{-d/\lambda_j \cos\theta} \quad (2)$$

where I_i° = signal intensity arising from overlayer core levels (i); I_j^{s} = signal intensity arising from substrate core levels (j); $f_i(\theta)$, $f_j(\theta)$ = signal intensity as a function of (θ) for core levels (i) and (j); F = X-ray flux, unattenuated over the sampling depth; α_i, α_j = cross section for photoionization of core levels (i) and (j); N_i, N_j = number of atoms per unit volume on which core levels (i) and (j) are localized; k_i, k_j = spectrometer factor for core levels (i) and (j); λ_i, λ_j = electron mean free path for core levels (i) and (j); d = overlayer thickness; and θ = angle between normal to sample surface and electron optics of energy analyzer.

Equations 1 and 2 can be simplified to treat the continuous overlayer model (Figure 7a). In this model, the substrate is covered with a continuous overlayer of thickness d, and the predicted intensities of the core-level signals from the overlayer and substrate are given in eq 3 and 4, respectively.

$$I_o = f(\theta)I_o^{\infty}(1 - e^{-d/\lambda_o \cos\theta}) \quad (3)$$

$$I_s = f(\theta)I_s^{\infty} e^{-d/\lambda_s \cos\theta} \quad (4)$$

In the case of the discontinuous models (Figure 7b,c,d), there is no continuous overlayer but, instead, both components in the system reside at the surface and occupy some fractional area coverage, Δ. These models result in the predicted core level signal intensities shown in eq 5 and 6.[5]

$$I_o = f(\theta)[\Delta I_o^{\infty}(1 - e^{-d/\lambda_o \cos\theta})] \quad (5)$$

$$I_s = f(\theta)[(1 - \Delta)_s^{\infty} + \Delta I_s^{\infty} e^{-d/\lambda_s \cos\theta}] \quad (6)$$

Although the intensities in eq 5 and 6 are labeled substrate and overlayer, it should be clear that in the discontinuous models there is no clearly defined overlayer and substrate. Therefore, eq 5 and 6 should be regarded as the predicted signal intensities of each of the components in the system. For consistency among eq 3–6 and Figure 7, we will consider I_o as the signal from PS and I_s as the PEO signal intensity. The significantly lower solid state surface tension of PS (36 dyn/cm) compared to PEO (44 dyn/cm) and our experimental results showing a surface excess of PS are the basis for this assignment.

Let us first consider the continuous overlayer model. If the overlayer thickness d is small compared to the sampling depth (with known electron mean free paths, λ), the signal intensity for the PS overlayer is predicted to increase exponentially with increasing angle θ. Conversely, the signal intensity from the PEO substrate is predicted to decrease exponentially. If, however, d is larger than the sampling depth, then only the C_{1s} signal from PS will be observed, and it will not show angular dependence. In addition, this model predicts that the C_{1s}(PEO)/O_{1s}(PEO) signal intensity ratio for the PEO component will increase because of the differences in electron mean free paths from these levels, $\lambda(C_{1s}) > \lambda(O_{1s})$.

Our experimental results are not consistent with the continuous overlayer model. The data in Table III show the presence of both components in the surface layer probed by XPS. We also found, with a single exception, that the C_{1s}(PEO)/O_{1s}(PEO) signal intensity ratio remained invariant with angle, θ. This result clearly indicates that PEO is not covered by PS. If PEO is, therefore, exposed at the air–solid interface and the C_{1s}/O_{1s} ratio is not angular dependent, then the PEO must be arranged morphologically in the copolymer in such a manner that its thickness is large compared to the XPS sampling depth. Finally, the [XPS(θ)] data shown in Figure 6 and Table III depict a small, gradual increase in PS concentration with increasing angle θ rather than the predicted exponential increase.

Having demonstrated that our experimental results are not consistent with the classic overlayer model, let us now consider the alternative discontinuous models shown in Figure 7 and described by eq 5 and 6. The model shown in Figure 7b has discontinuous islands of PS at the surface and the thickness d of these islands is less than the XPS sampling depth of ~50 Å. With this model, and eq 5 and 6, an exponential increase in PS signal intensity, relative to the PEO, is predicted as angle θ is increased where a plateau value would be reached corresponding to the first term in eq 6. Our data in Table III show either no increase or a small increase in PS signal intensity as θ is increased; therefore, this model does not fit the experimental results.

The models shown in Figure 7c,d are similar in many respects, but they predict slightly different angular dependencies for the PS component at large angles of θ. In these models both components are exposed at the surface, and they are organized into domains that are thick compared to the XPS sampling depth. This makes both models consistent with our observation that the C_{1s}-(PEO)/O_{1s}(PEO) signal intensity ratio for PEO in the copolymer is invariant with angle θ. The major difference between the models shown in Figure 7c,d is that in the latter model, the PS domains are slightly raised above the PEO domains at the surface, thus effectively "shadowing" the PEO at high take-off angles, θ. This difference is

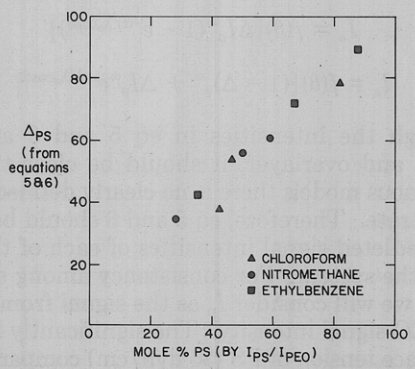

Figure 8. Surface copolymer composition determined by XPS vs. fractional area coverage, Δ, determined from eq 5 and 6 for copolymers cast from chloroform, ethylbenzene, and nitromethane.

significant because the model in Figure 7c is predicted to have no angular dependence in the PS and PEO signal intensities whereas the model in Figure 7d is expected to show a relative increase in the PS signal intensity at large values of θ. Data in Table III can be selected to support both of these models, but there is more evidence in favor of the model shown in Figure 7d. Copolymer films cast from chloroform, a mutual solvent for PS and PEO, clearly fit the model shown in Figure 7d whereas copolymers cast from preferential solvents for the major component in the copolymer appear to behave like the model structure shown in Figure 7c.

Having established the general topography of the block copolymer films, we can now use eq 5 and 6 to calculate Δ and (1 − Δ), the fractional surface areas occupied by the PS and PEO components, respectively. The experimentally measured intensity ratios for the PS (I_o/I_o^∞) and PEO (I_s/I_s^∞) components in the copolymers were substituted into eq 5 and 6 and values of Δ and (1 − Δ) were calculated for the three block copolymers cast from ethylbenzene, nitromethane, and chloroform. The results are shown in Figure 8 where Δ is plotted against the molar composition of the surface (mol % PS) determined by XPS and previously shown in Figure 4. Figure 8 shows a remarkable correlation between the two values, thus indicating that the fractional surface area occupied by the copolymer components is proportional to the composition of the copolymer at the surface.

It would be of considerable interest to be able to correlate surface morphologies determined by electron microscopy with surface topographies determined by XPS. This has not been done systematically; however, we are encouraged by the results of the investigation of one particular case. Shown in Figure 9 is a replication electron micrograph[6] of a free surface made from a film of copolymer A (rich in PEO) cast from nitromethane, a preferential solvent for PEO. Globules of PS decorate the surface of the fibrillar PEO component in the copolymer. A comparison of the area ratio of the PS globules to the PEO continuous phase averaged over the entire micrograph (e.g., within and outside the sheaf) reveals ~27% of the surface is occupied by the PS globules. From Table III, one finds that XPS measurements show a surface composition of 28 mol % PS. The shadowing of the edges of the PS domains from the replication electron micrograph, Figure 9, indicates that the PS globules are slightly raised above the PEO continuous phase. These two morphological observations are consistent with the model developed from XPS(θ) studies on the PS/PEO system.

Conclusions

XPS was used to determine the surface composition and topography of PS–PEO block copolymer films having

Figure 9. Replication electron micrograph of free surface of copolymer A cast from nitromethane. Reprinted with permission from ref 6. Copyright 1970 Plenum Press.

different chemical compositions and cast from selective and mutual solvents. From our experimental results, and a proposed model for the surface, we conclude that:

1. The surfaces of all the solvent cast copolymer films are significantly richer in PS than is the bulk.
2. The concentration of PS at the surface of a given copolymer is solvent dependent and the trends follow the order ethylbenzene > chloroform > nitromethane.
3. The copolymer surfaces are laterally inhomogeneous in PS and PEO and the PS component is often raised above the PEO component (nonplanar).
4. The morphology consists of isolated domains of each component extended into the surface to depths greater than 50 Å.
5. The molar composition at the copolymer surface determined by XPS corresponds to the surface area occupied by each copolymer component.

The work reported here illustrates the vast potential of the use of detailed angular-dependent XPS studies on the surfaces of block copolymer systems. In this particular case, a quantitative and qualitative description of the surface was possible and the technique of [XPS(θ)] is being applied to other block copolymer systems as well as homopolymer and copolymer blends in an attempt to obtain a clear picture of the surface structure and bonding in polymer systems in general.

Acknowledgment. We wish to thank Drs. Salaneck, Beatty, and Davidson of Xerox Corporation and Drs. Dilks and Clark of the University of Durham (U.K.) for helpful discussions. We also wish to extend our thanks to Barbara

H. Fornalik for typing the manuscript.

References and Notes

(1) D. T. Clark, "Chemical Applications of ESCA in Electron Spectroscopy", W. Dekeyser, Ed., D. Reidel Publishing Co., Dordrecht, Holland, 1973 (NATO Summer School Lectures, Ghent, September 1972).
(2) D. T. Clark, "Structure and Bonding In Polymers Revealed by ESCA In Electronic Structure of Polymers and Molecular Crystals", L. J. Andre, Ed., Plenum Press, New York, N.Y., 1975 (NATO Summer School Lectures, Namur, September 1974).
(3) D. T. Clark, "Advances in Polymer Sciences", Vol. 24, H.-J. Cantow et al., Eds., Springer-Verlag, Berlin, 1977, p 126.
(4) K. Siegbahn, C. Nordling, A. Fahlman, R. Nordberg, K. Hamrin, J. Hedman, G. Johansson, T. Berkmark, S. E. Karlsson, I. Lindgren, and B. Lindberg, "ESCA, Atomic, Molecular and Solid State Structure Studied by Means of Electron Spectroscopy", Almquist and Wiksells, Uppsala, 1967.
(5) D. T. Clark and H. R. Thomas, *J. Polym. Sci., Polym. Chem. Ed.*, **15**, 2843 (1977).
(6) R. G. Crystal, P. F. Erhardt, and J. J. O'Malley in "Block Copolymers", S. L. Aggarwal, Ed., Plenum Press, New York, N.Y., (1970), pp 179–193 and references therein.
(7) J. M. Short and R. G. Crystal, *Appl. Polym. Symp.*, **16**, 137 (1971).
(8) L. H. Lee, *Adv. Chem. Ser.*, **87**, 106 (1968).
(9) J. J. O'Malley, R. G. Crystal, and P. F. Erhardt, ref 6, pp 163–178.
(10) D. T. Clark, H. R. Thomas, A. Dilks, and D. Shuttleworth, *J. Electron Spectrosc. Relat. Phenom.*, **10**, 455 (1977).
(11) D. T. Clark and H. R. Thomas, *J. Polym. Sci., Polym. Chem. Ed.*, **14**, 1671 (1976).
(12) D. T. Clark in "Progress in Theoretical Organic Chemistry", Vol. 2, I. G. Csizmadia, Ed., Elsevier, Amsterdam, 1976.
(13) D. T. Clark, D. B. Adams, I. W. Scanlan, and I. S. Woolsey, *Chem. Phys. Lett.*, **25**, 263 (1974).
(14) D. T. Clark and D. B. Adams, *J. Electron Spectrosc. Relat. Phenom.*, **7**, 401 (1975).
(15) D. T. Clark, A. Dilks, J. Peeling, and H. R. Thomas, *Faraday Discuss. Chem. Soc.*, **60**, 183 (1975).
(16) D. T. Clark, D. B. Adams, A. Dilks, J. Peeling, and H. R. Thomas, *J. Electron Spectrosc. Relat. Phenom.*, **8**, 51 (1976).
(17) R. Manne and T. Aberg, *Chem. Phys. Lett.*, **7**, 282 (1970).
(18) J. H. Scofield, *J. Electron Spectrosc. Relat. Phenom.*, **8**, 129 (1976).
(19) D. T. Clark and H. R. Thomas, *J. Polym. Sci., Polym. Chem. Ed.*, **16**, 791 (1978).
(20) C. S. Fadley, R. J. Baird, W. Siekhaus, T. Novakov, and S. Å. A. Biegstrom, *J. Electron Spectrosc. Relat. Phenom.*, **4**, 93 (1974).
(21) B. L. Henke, *Adv. X-Ray Anal.*, **13**, 1 (1969).
(22) B. L. Henke, *J. Phys. C*, **4**, 115 (1971).

Photon Correlation Spectroscopy of Polystyrene in the Glass Transition Region

H. Lee, A. M. Jamieson,* and R. Simha

Department of Macromolecular Science, Case Western Reserve University, Cleveland, Ohio 44106. *Received December 11, 1978*

ABSTRACT: The dynamic characteristics of the light scattered by atactic polystyrene in the temperature range 92–110 °C are determined by digital photon correlation spectroscopy. Two discrete relaxation processes are present. A slow mode can be represented by an asymmetric Williams–Watts distribution of relaxation times and is essentially identical to that observed by Patterson et al. in the depolarized light-scattering spectrum. A fast process is well defined by a single exponential decay. The characteristic mean relaxation times are compared with the conventional relaxation map for polystyrene, as obtained by dynamic mechanical and dielectric techniques. Concordance between mechanical and photon correlation results in respect to the glass transition process is observed. While the activation energies are also identical with those derived from dielectric data, the characteristic frequencies are lower by two orders of magnitude. As for the β process, the derived activation energy of about 15 kcal/mol is in the range of general expectation, but lower by a factor of 2 than most of the mechanical information reported in the literature. Photon correlation techniques employing both the anisotropic and isotropic components appear to be powerful tools for dynamic relaxation spectroscopy in the glassy state.

Photon correlation spectroscopy has become a well-established technique for examining the hydrodynamic behavior of concentration fluctuations in polymer solutions.[1-5] Subsequently, investigators have successfully applied this probe to study the dynamics of structural relaxation in viscous liquids[6] and inorganic glasses.[7,8] More recently, interest has developed in applying the method to characterize the relaxational behavior of configurational fluctuations of bulk polymers.[9-11] Discrete fast and slow exponential decay processes have been reported in the isotropic light-scattering component of poly(methyl methylacrylate).[9,10] It was concluded that the slow process is related to the glass transition relaxation, while the fast mode is due to side-chain reorientation.[9,10] The depolarized Rayleigh spectrum of polystyrene in the melt near the glass transition temperature has been extensively studied by Patterson et al.[11] A very wide distribution of relaxation times covering five decades of time is observed which is accurately characterized by the Williams–Watts function[12]

$$\phi(t) = \alpha \exp[-(t/\tau_0)^{\beta}] \quad (1)$$

where α, τ_0, and $0 < \beta \leq 1$ are adjustable parameters. The depolarized spectrum of polystyrene is characterized by an average relaxation time and an activation energy which are stated to be in the range observed by other dynamic relaxation methods for the glass–rubber transition in polystyrene.[11]

In this paper we report a study of the relaxation spectrum of the total intensity of light scattered by polystyrene over a similar range of temperatures. In these experiments, we detect the superposition of the isotropic and depolarized scattering components. Two discrete relaxation modes appear to be present: a slow mode identical to that reported by Patterson et al.,[11] and a single exponential decay which is two orders of magnitude faster than the former.

Experimental Section

(a) Sample Preparation. Monomer styrene was obtained from Aldrich Chemical Co., containing 10–15 ppm of *p-tert*-butylcatechol as inhibitor. The latter was removed by washing with aliquots of 20% NaOH solution and water, and the monomer

0024-9297/79/2212-0329$01.00/0 © 1979 American Chemical Society